

Magnetic-Tuning Millimeter-Wave CMOS Oscillators

(Invited Paper)

Xiaolong Liu¹, Zhiqiang Huang², Jun Yin³ and Howard C. Luong¹

¹Hong Kong University of Science and Technology, Clear Water Bay, Hong Kong

²Samsung Semiconductor, San Jose, CA

³University of Macau, Macau

Abstract—This paper demonstrates that magnetic tuning can be employed either as coarse tuning or fine tuning or both for mm-Wave fundamental oscillators to achieve ultra-wide frequency tuning range and low phase noise. Firstly, a multi-mode VCO with a tuning range of 41.1% from 57.5 GHz to 90.1 GHz with phase noise of -111.8 dBc/Hz at 10-MHz offset and FoM_T of -192.2 dBc/Hz is discussed. Secondly, a dual-band varactor-less DB-VCO with 14.3% tuning range from 95.7 GHz to 110.5 GHz and -106.9 dBc/Hz phase noise at 10-MHz offset is presented together with a quad-band varactor-less QB-VCO achieving a tuning range of 32% from 58.8 GHz to 81.2 GHz and phase noise of -115.8 dBc/Hz at 10-MHz offset and FoM_T of -192.4 dBc/Hz. Finally, a 95-GHz DCO provides a tuning range of 27% is demonstrated. It achieves a phase noise of -110 dBc/Hz at 10-MHz offset and FoM_T of -186.1 dBc/Hz.

Keywords—mm-Wave, magnetic tuning, CMOS, VCO, DCO, tuning range, phase noise, transformer, tank Q , varactor-less

I. INTRODUCTION

Millimeter-wave (mm-Wave) frequencies from 60-to-110 GHz can be utilized for various useful and interesting applications, including high-data-rate short-range wireless backhaul, high-resolution vehicular radar, high-sensitivity medical and security imaging [1-3]. These applications rely on stringent specifications not only on the transceiver's broadband operation but also on the transmitter's error vector magnitude (EVM) and on the receiver's signal-to-noise ratio (SNR), which in turn impose challenging requirements of LO signals in term of ultra-wide frequency tuning range and good phase noise, in particular in CMOS processes [4]-[5]. Firstly, at mm-Wave frequencies, the parasitic become relatively large as compared to the tank capacitor and significantly degrade the frequency tuning range. Secondly, the quality factor Q of varactors becomes dominantly low (<3 at 100 GHz). Thirdly, the trade-off between the tuning range and the phase noise becomes more severe. With the same target power consumption and phase noise, the degraded varactor Q at mm-Wave frequencies would inevitably limit the frequency tuning range to ~15% [6]-[7].

As alternative solutions, interpolative-phase-tuning or rotated-phase-tuning technique was proposed for varactor-less mm-Wave oscillators to improve the phase noise in [8]-[9]. However, multiple dedicated phase shifters are required in [8], resulting in high power consumption, and in [9], there exists a severe trade-off between the tuning range and the phase error of the multi-phase LC oscillator. Moreover, for these oscillators, the frequency tuning is done by intentional shifting of the operation frequency from the resonant peak frequency of

the LC tank through injected current, which unfortunately degrades the tank Q and results in a steep frequency response.

Over the years, magnetic tuning has been used to extend the tuning range of RF and mm-Wave LC oscillators [10-24]. Specifically, magnetic tuning can be achieved by switching on/off extra coupled coils relative to the primary resonant coil for coarse tuning as in [10-18], by continuously changing the current [19-23] or continuously varying the loaded resistor [24] in the secondary coil of a transformer for fine tuning. With proper design of switched inductors, the effective turn-on resistance and turn-off parasitic capacitance of the switches contributed to the resonant coil are significantly reduced due to the relative small coupling coefficients between these coupled coils. As a consequence, magnetic tuning can be employed to improve the frequency tuning range while minimizing the phase noise degradation.

A magnetic-tuning VCO with two extra coupled switched-inductors achieves an ultra-wideband tuning range of 61.9% at a center frequency of 11.75 GHz in [10]. However, applying the same idea to mm-Wave frequencies, the frequency tuning range would be less than ~28% due to more dominant parasitic from the active devices and switches [11-13]. In [18], a switched-triple-shielded transformer-based magnetic-tuning oscillator measures a record ultra-wide tuning range of 41.1% at a center frequency of 73.8 GHz. However, all these mm-Wave magnetic-tuning oscillators [11-18] still suffer from the problem of relying on low- Q varactors for fine tuning.

Another way to extend the coarse tuning range of mm-Wave oscillators is to employ high-order LC tanks with dual-resonant modes [25-29] or three-resonant modes [30]. However, their frequency tuning range is still limited. Harmonic extraction [31]-[32] or self-mixing [33] oscillators can benefit from wide tuning range and low phase noise, but at the cost of much lower output power and thus much higher power consumption.

In order to avoid using low- Q varactors for fine tuning at mm-Wave frequencies, magnetic tuning by continuously changing the current or resistor at the secondary coil is a good candidate. In [19], by varying the bias current and thus the transconductance (g_m), the impedance seen from the resonant coil is continuously tuned. However, a small resistor is needed to shunt with the resonant inductor to ensure linear change of the effective inductance over a wide tuning range, resulting low tank Q . In [20], the currents in the coupling coils are forced to be in-phase or out-of-phase by a quadrature oscillator topology, and by defining their relative amplitude, the oscillate frequency is varied. In [21], evolved from [19], a bimodal

enhanced-magnetic-tuning technique is proposed to further extend the tuning range of mm-Wave quadrature oscillators to 24%. However, as the frequency tuning depends on changing bias currents, these works [20]-[21] need to consume large power up to 30 mW for wide tuning range. The technique is also leveraged for 100-GHz [22] and 200-GHz [23] oscillators for the applications at sub-Terahertz (sub-THz) frequencies, but with limited tuning range of 11.2% and 3.5%, respectively, mainly due to limited current range available without contributing too much parasitic. Compared to the magnetic fine tuning with continuously controlling the current, the method with a loaded continuously variable resistor [24] do not need to burn more power for fine tuning. However, [24] has a smaller tuning range of 16% at 60 GHz due to limited frequency tuning bands.

This paper discusses and demonstrates mm-Wave oscillators employing magnetic tuning technique for both coarse and fine tuning to achieve ultra-wide tuning range, low phase noise, and low power consumption. Firstly, a switched-triple-shielded transformer is proposed to coarsely change the coupling coefficients between the primary and secondary coils in a dual-resonate tank to greatly increase the frequency tuning range of a mm-Wave VCO to cover a frequency range from 57.5-to-90.1 GHz. Secondly, multiple mode varactor-less mm-Wave VCOs are proposed with a triple-coil transformer and a switched-quadruple-shielded transformer to achieve frequency tuning range from 95.7-to-110.5 GHz and 58.8-to-81.2 GHz, respectively. Finally, a split transformer with multiple non-uniform secondary coils is proposed as the variable inductor for a DCO to cover a tuning range from 82-to-107.6 GHz while maximizing the tank Q for good phase noise.

II. MAGNETIC-TUNING FOR MULTI-MODE VCO

The conventional method to increase the frequency tuning range while still keeping small chip area is using transformer-based dual-band VCO [25-26]. Unfortunately, it can only provide two frequency tuning bands and each band still has limited tuning range due to varactor tuning at mm-Wave frequencies. In order to further extend the tuning range by creating more frequency tuning bands without degrading the tank Q , a magnetically-tuned multi-mode VCO with tunable coupling coefficient K_{12} was proposed as shown in Fig.1(a), and its fully schematic is shown in Fig. 4 [18], [34]. As illustrated in Fig. 1(b), the impedance seen from either coil has two distinct frequency peaks, which allows VCO oscillating at two different frequencies by turning on one of the tail-current sources I_1 or I_2 . The oscillation frequencies for two different bands can be expressed as [26]:

$$\hat{\omega}_1^2 = \frac{\omega_1^2 + \omega_2^2 + \sqrt{(\omega_1^2 - \omega_2^2)^2 + 4K_{12}^2 \omega_1^2 \omega_2^2}}{2(1 - K_{12}^2)} \quad (1a)$$

$$\hat{\omega}_2^2 = \frac{\omega_1^2 + \omega_2^2 - \sqrt{(\omega_1^2 - \omega_2^2)^2 + 4K_{12}^2 \omega_1^2 \omega_2^2}}{2(1 - K_{12}^2)} \quad (1b)$$

where $\omega_1 = (L_1 C_1)^{-1/2}$ and $\omega_2 = (L_2 C_2)^{-1/2}$. From (1a) and (1b), both the oscillation frequencies ω_H and ω_L depend on the coupling coefficient K_{12} , which provides another degree of freedom to tune the frequency. Fig. 2 plots the relationships between ω_L (ω_H) and K_{12} for different ω_2/ω_1 ratios. From both (1a) and Fig. 2, it is clear that ω_H is quite sensitive to the coupling coefficient K_{12} , especially when K_{12} is above 0.5.

Now the challenge is how to tune the coupling coefficient K_{12} . The simplest way is to add a switching coil to change the coupling coefficient between the original two coils. Fig. 3 shows a multiple-port transformer layout with the proposed tuning scheme of K_{12} . Intuitively, when M_{S1} turns on, the current i_1 in L_1 induces a current i'_{sh1} in L_{sh1} and another current i'_2 in L_2 , both of which are in the opposite direction with i_1 . Since i'_{sh1} also in turn induces another current i''_2 in L_2 , which tends to cancel i'_2 , the effective coupling coefficient $K_{12,eq}$ between L_1 and L_2 actually becomes lowered as compared with the case when M_{S1} turns off [35]. In this case, K_{12} becomes tunable by switching the M_{S1} on and off.

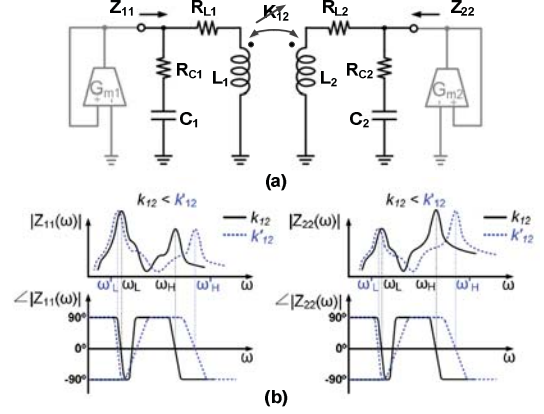


Fig. 1. Magnetically-tuned dual-band VCO: (a) model and (b) amplitude and phase response of the tank impedance with different coupling coefficient K_{12}

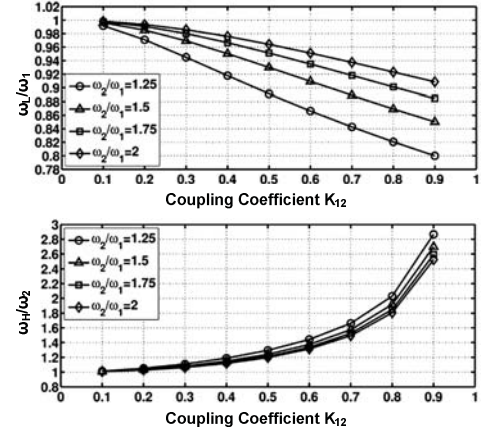


Fig. 2. Calculated resonant frequencies ω_H and ω_L as functions of the magnetic coupling coefficient K_{12} for different ω_2/ω_1 ratios

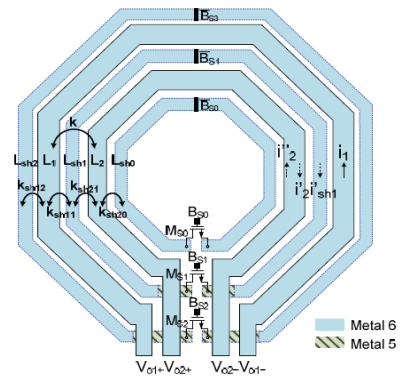


Fig. 3. Transformer structure for the proposed tuning scheme of the magnetic coupling coefficient K

Because the effective inductances of L_1 and L_2 are also changed when M_{S1} turns on and off, two additional shielding coils L_{sh0} and L_{sh2} with the series switches M_{S0} and M_{S2} are added. When M_{S1} is off, both M_{S0} and M_{S2} are turned on, L_{sh0} and L_{sh2} introduce counteractive currents in L_1 and L_2 to prevent increase in inductance for L_1 and L_2 . Similarly, when M_{S1} is on, both M_{S0} and M_{S2} are turned off to avoid decrease in inductance for L_1 and L_2 . As a result, the equivalent inductances of L_1 or L_2 are kept relatively constant when M_{S1} turns on and off to tune K_{12} . With the two extra switched coils, more tuning modes can also be created as shown in Table I. Fig. 5 shows the measured phase noise at 10-MHz offset from -104.6 dBc/Hz to -112.2 dBc/Hz across the whole frequency tuning range of 41.1% from 57.5 GHz to 90.1 GHz.

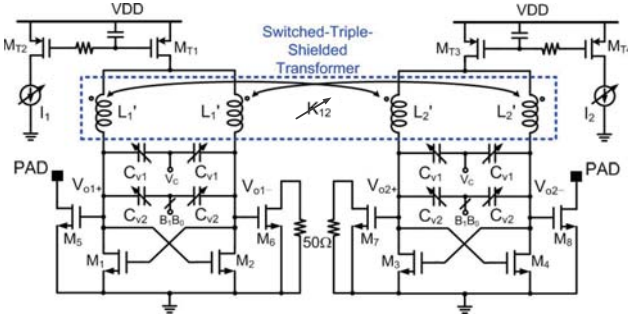


Fig. 4. Schematic of the proposed multi-mode dual-band VCO [18]

TABLE I MODES SELECTION CONTROL LOGICS

	Mode 1	Mode 2	Mode 3	Mode 4	Mode 5	Mode 6
$B_{S2}B_{S1}B_{S0}$	101	011	111	010	001	111
I_1	on	on	on	off	off	off
I_2	off	off	off	on	on	on

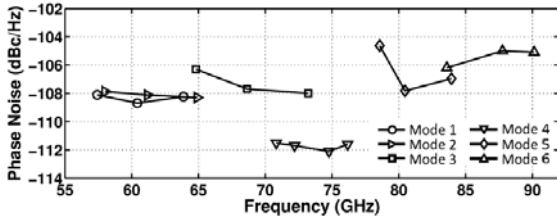


Fig. 5. Measured VCO phase noise at 10-MHz offset frequency across the entire frequency tuning range

III. MAGNETIC-TUNING FOR VARACTOR-LESS OSCILLATORS

Although the magnetically-tuned multi-mode VCO can offer ultra-wide tuning range of 41.1% [18], it only has a few coarse tuning bands and still requires wide-tuning-range capacitance tuning using varactors for fine tuning to cover frequency gaps, which would inevitably degrade the tank Q , the start-up condition, the phase noise, and the operation frequency. As aforementioned, the varactor Q decreases quickly with the frequency. For instance, using a varactor to achieve $\sim 10\%$ tuning range without consideration of other parasitic, as shown in the Fig. 6, the simulated worst-case varactor Q drops from 7 at 30 GHz to only 2 at 120 GHz in a standard 65nm CMOS process. At 100 GHz, with a change of the control voltage from 0 V to 1.2 V, the varactor can be tuned from 9 fF to 4 fF, while the varactor Q varies from 2.5 to 6. Although the inductor Q is very high (~ 35), the tank Q would be unacceptably small with the low- Q varactor. To tackle this issue, continuous tuning of magnetic field can be adopted as fine tuning to eliminate low- Q varactors.

A. Fine Magnetic Tuning

The variable inductor using a transformer with a continuously-tuned variable resistor can provide continuous frequency tuning without adding capacitor to the tank, as shown in Fig. 7(a) [24]. The input impedance of the resonant coil L_1 can be derived as:

$$Z_{11} = R_{L1} + j\omega L_1 + \frac{\omega^2 K_{12}^2 L_1 L_2}{R_{L2} + j\omega L_2 + R_V / (1 + j\omega R_V C_V)} \quad (2)$$

The effective inductance $L_{1,eq}$ and the equivalent resistive loss $R_{L1,eq}$ can be derived by extracting the real and imaginary parts of Z_{11} , from which the tank Q is ready to be calculated as:

$$Q_{1,eq} = \frac{\alpha L_{1,eq}}{R_{L1,eq}} = \frac{\omega \beta L_1 - \omega^3 K_{12}^2 L_1 L_2 (L_2 - \alpha R_V C_V)}{\beta R_{L1} + \omega^2 K_{12}^2 L_1 L_2 (R_V + \alpha)} \quad (3)$$

where $\alpha = R_V / (1 + \omega^2 R_V^2 C_V^2)$, $\beta = (R_{L2} + \alpha^2)^2 + \omega^2 (L_2 - \alpha R_V C_V)^2$. For a simplified case, assuming only variable resistor R_V is included, the simulated tank inductance $L_{1,eq}$ is shown in Fig. 7(b). The tuning range (TR) of inductance is given as [36]:

$$TR = \frac{\Delta L_{1,eq}}{L_1} \approx \frac{M^2}{L_1 L_2} = K_{12}^2 \quad (4)$$

Fig. 7(c) shows the simulated tank Q at 100 GHz versus the tuning variable resistor R_V . When the variable resistor is tuned to match the output impedance of secondary coil, the quality factor is the lowest with a value of Q_{min} [36]:

$$Q_{min} \approx \frac{2}{K_{12}^2} - 1 = \frac{2}{TR} - 1 \quad (5)$$

When its coupling factor K_{12} is increased to achieve a wider tuning range, more loss is introduced from the variable resistor to the primary coils and further degrades the tank Q .

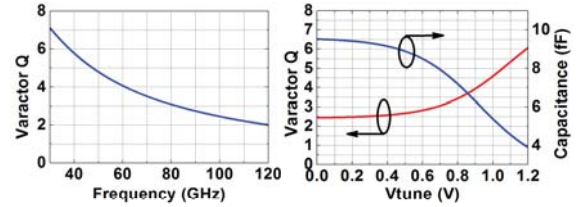


Fig. 6. Simulated varactor Q with frequency and control voltage at 100 GHz

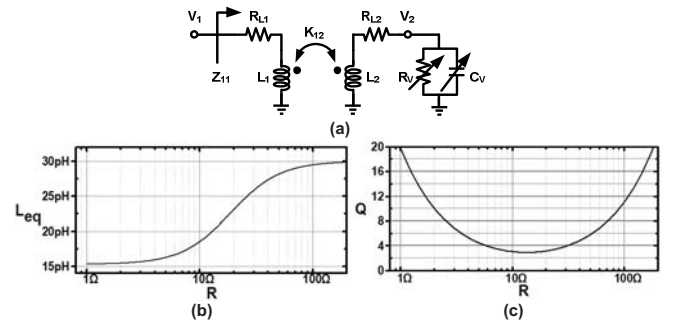


Fig. 7. (a) Magnetic tuning using a transformer and variable resistor R_V , and its equivalent circuit, (b) the simulated tank inductance $L_{1,eq}$, and (c) the simulated tank Q at 100 GHz versus resistor R_V ($L_1=L_2=30$ pH, $K_{12}=0.7$)

B. 103-GHz Varactor-Less Dual-Band VCO

In order to improve the tuning range and tank Q , magnetic tuning techniques for both coarse and fine frequency tuning are applied for a dual-band VCO. As shown in Fig. 8 [37], turning

a QB-VCO with a switched-quadruple-shielded transformer, as shown in Fig. 12 [38].

The operation of the proposed QB-VCO can be divided into two modes. When only the bias current I_{B1} is on, the VCO operates in the high-frequency mode. On the other hand, when only I_{B2} is on, the VCO operates in the low-frequency mode. In each mode, a continuously controlled variable resistor M_{S1} (M_{S2}) is used for continuous magnetic and frequency tuning, while a discretely-controlled switch M_{S3} (M_{S4}) is used for coarse magnetic and frequency tuning. As a compromise between the tank Q and the tuning range, M_{S1} and M_{S3} are sized so that their turn-on resistances for fine tuning and coarse tuning are $\sim 9 \Omega$ and $\sim 15 \Omega$, respectively, to ensure acceptable weak degradation of the tank Q . The same consideration is also applied for switches M_{S2} and M_{S4} .

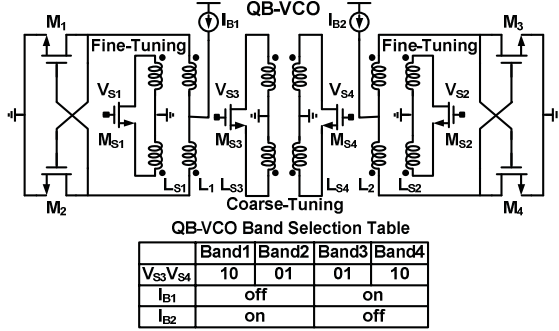


Fig. 12. The schematic of the proposed quad-band VCO

To guarantee the stability of the proposed dual-mode QB-VCO, the coarse magnetic tuning coil L_{S3} and L_{S4} are also reconfigurable as the shielded coil to reduce the coupling coefficient between the resonator coils L_1 and L_2 [35]. Only either of L_{S3} and L_{S4} is shorted at any time, as the selection table shown in Fig. 12. Simulated with ADS momentum, the equivalent inductance can be continuously tuned from 39 pH to 77 pH, and the tank Q is above 6 over the entire frequency range, as shown in Fig. 13(b).

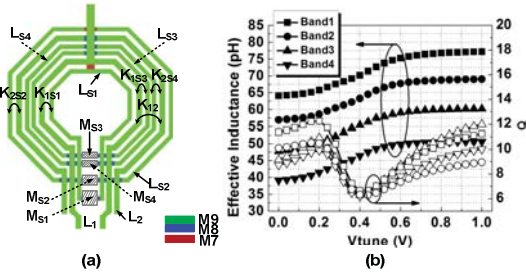


Fig. 13. (a) Layout of the proposed six-coil transformer and (b) simulated equivalent inductance and tank Q vs. the fine tuning control voltage

This switched-quadruple-shielded transformer in Fig. 13(a) seems similar as the switched-triple-shielded transformer in Fig. 3 [18], but there has some fundamental differences and features: 1) the coarse tuning is achieved by varying the effective $L_{1,eq}/L_{2,eq}$ and keep the effective $K_{12,eq}$ almost constant in this work, while is achieved by changing the effective $K_{12,eq}$ and keeping the effective $L_{1,eq}/L_{2,eq}$ almost constant in [18]; 2) the shielded coils L_{S1} and L_{S2} are used for fine tuning and none additional varactors are needed in this work, while the shielded coils L_{S1} and L_{S2} are employed to keep the effective $L_{1,eq}/L_{2,eq}$ constant and still need varactors for fine tuning in [18]. 3) The frequency tuning is not obvious by tuning the K_{12} in the low-frequency-band as shown in Fig.2

and results too much frequency overlap in Mode 1 and Mode 2 as shown in Fig. 5 [18], while the magnetic tuning is uniform in this work, as shown in Fig. 16.

D. Measurement Results

Fig. 14 shows the output spectrum and phase noise of the DB-VCO at frequency of 110.5 GHz, measuring -83.1 dBc/Hz and -102.2 dBc/Hz at 1-MHz and 10-MHz offsets, respectively. As shown in Fig. 15, the frequency tuning range is 14.3% from 95.7 GHz to 110.5 GHz, and the phase noise is from -100.6 to -106.9 dBc/Hz at 10-MHz offset.

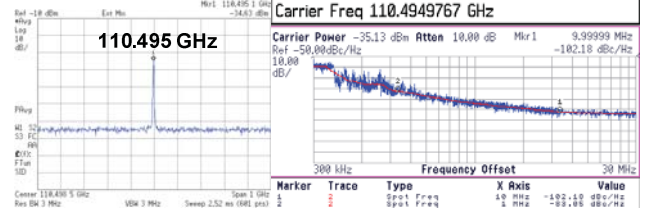


Fig. 14. Output spectrum and measured phase noise at 110.49 GHz

From Fig. 16, the QB-VCO measures a continuous frequency tuning range from 58.8 GHz to 81.2 GHz with phase noise of -93.3 dBc/Hz and -115.8 dBc/Hz at 1-MHz and 10-MHz offsets at 66.5 GHz, respectively. The measured phase noise across the entire frequency tuning range is from -103.6 dBc/Hz to -115.8 dBc/Hz at 10-MHz offset.

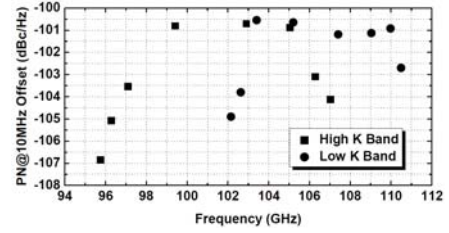


Fig. 15. Measured phase noise across the tuning range

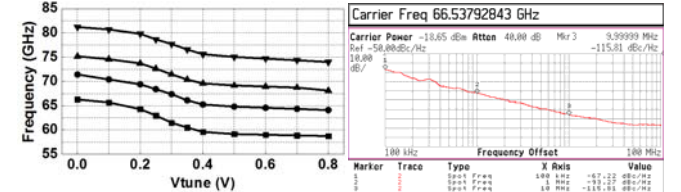


Fig. 16. Measured frequency tuning range of the QB-VCO and measured phase noise at 66.5 GHz

IV. MAGNETIC-TUNING WITH SPLIT TRANSFORMER

Because of smaller tank capacitance, the variable inductor [24] can oscillate at high frequencies. But the most critical issue is the quality factor degradation when it is designed for wide tuning range. In order to minimize the Q degradation, a split transformer with multiple secondary coils is proposed as the variable inductor, as shown in Fig. 17 [36]. The proposed split transformer consists of two parallel transformers L_a and L_b , each of which is designed to have 3 parallel secondary coils with small coupling factor K_i to maximize $Q_{min,i}$. Theoretically, the minimum quality factor contributed by each variable resistor is $Q_{min} \approx \frac{2N}{TR} - 1$, where N is the total number of secondary coils and each coil is sized uniformly with a tuning range of $\frac{TR}{N}$.

This technique may look similar to the switched-transformer with variable inductor [37], which creates

multiple-bands to reduce tuning range requirement of variable inductor. However, the proposed split-transformer with multiple variable resistors has no frequency gap issue as in the conventional switched transformer. For the conventional tuning in Fig. 18(a), the control signals (R_V , D) need to be switched from ($R_V=\infty$, $D=0$) to ($R_V=0$, $D=1$) for further tuning in another band after the frequency is continuously tuned down from $f(R_V=0, D=0)$ to $f(R_V=\infty, D=0)$. With PVT variation, $f(R_V=\infty, D=0)$ can be higher than $f(R_V=0, D=1)$, resulting in a frequency gap. However, the proposed tuning scheme in Fig. 18(b) can use R_{V2} for further tuning in another band without switching the control signals, which guarantees no frequency gap between adjacent tuning bands.

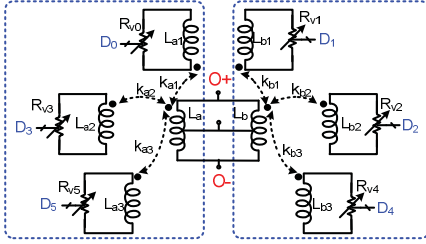


Fig. 17. Schematic of the proposed split transformer as variable inductor

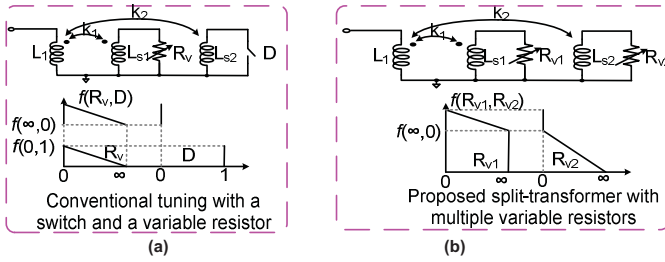


Fig. 18. Comparison of the frequency tuning for (a) the conventional tuning with a switch and a variable resistor [37] and (b) the proposed split-transformer with multiple variable resistors

The design considerations for the proposed split transformer include the following:

1) *Tuning range of each secondary coil*: When more variable resistors are turned on for higher frequencies, the overall Q would be degraded by on-resistance of the variable resistor. If the secondary coils are designed to be non-uniform, and if the secondary coil with a smaller tuning range is selected for tuning at a higher frequency, the split transformer can operate in the region with a higher Q . Besides, the non-uniform secondary coils can create more high- Q regions to reduce the Q degradation. As illustrated in Figs. 19(a) and 19(b), for f_1 , tuning R_{V2} first (Case 2) would result in a low- Q region whereas tuning R_{V1} first (Case 1) would operate the tank in a high- Q region. Similarly, for another target frequency f_2 , the tank can be operated in a high- Q region by swapping the tuning order from Case 1 to Case 2 with R_{V2} being tuned first. If the split transformer were designed uniformly, there would be no improvement by swapping the tuning order.

2) *Sizing of the variable resistor*: In order to minimize on-resistance to reduce the loss, the variable resistor should be sized larger. However, the parasitic capacitance would lower the self-resonant frequency and boost the amplitude at the secondary coil due to series LC peaking, introducing higher loss. Thus the variable resistors should be sized based on the trade-off between on-resistance and self-resonant frequency.

3) *Transformer structure and mutual coupling factors*:

Because the mutual coupling between the secondary coils could effectively provide a shielding effect and reduces the coupling factor to the primary coil when the secondary coils are turned on [35], the transformer structure design needs to minimize the mutual coupling. The transformer can be split into two parallel transformers L_a and L_b with similar structures to minimize the mutual coupling between secondary coils. As shown Fig. 20, the inner coils L_{a1} and L_{a2} are respectively coupled to the upper and lower parts of the primary coil L_a to minimize the overlap between L_{a1} and L_{a2} . The outer coil L_{a3} is placed away from L_{a1} and L_{a2} for smaller mutual coupling. Finally, a shorted coil surrounding L_{a3} is added to increase the self-resonant frequency.

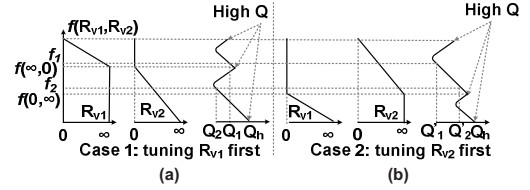


Fig. 19. The proposed split-transformer using swapping scheme with: (a) non-uniform tuning range with R_{V1} tuned first, (b) non-uniform tuning range with R_{V2} tuned first

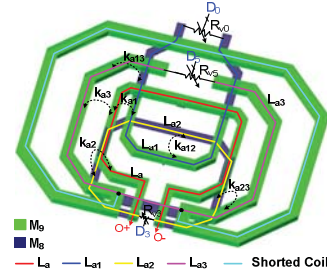


Fig. 20. Layout of the proposed split transformer L_a and its parameters

As shown in Fig. 21, when the number of secondary coils N is increased from 1 to 3 and 6, the W-band DCO with the proposed split-transformer has smaller start-up current and thus better tank Q , which verify the effectiveness of split-transformer. By swapping the tuning order, the start-up current degradation is further reduced. Thanks to the proposed split transformer, the W-band DCO achieves the widest tuning, of up to 27%, and the best worst-case FOM_T , as well as a comparable FoM among the existing 100-GHz oscillators.

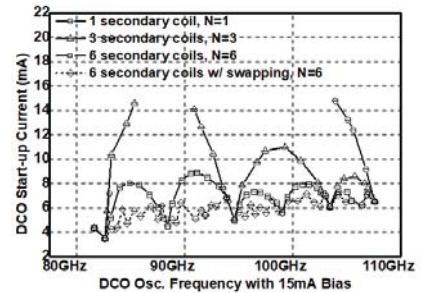


Fig. 21. Measurements of the proposed DCO start-up current versus the DCO frequency.

V. DESIGN OF MULTI-COIL TRANSFORMER

In this work, multi-coil transformers are the critical part for designing high performance mm-Wave oscillators. The loss and parasitic of the coils have big influence on the oscillator at mm-Wave frequencies. As such, it is very important to develop a custom procedure to improve the design efficiency and simulation accuracy. The simulation

accuracy mainly depends on the modeling of the multi-coil transformer because it is typically much easier and more accurate to extract the parasitic of the active devices and their interconnection. The design procedure and modeling of the multi-coil transformer can be recommended as follows.

1) Firstly, given the design specification, determine how many parallel secondary coils need to be used for coarse/fine magnetic tuning.

2) Derive the effective resonant inductance using a simplified equivalent circuit for the multi-coil transformer as in [18], [37]. With the help of mathematic assistant software, preliminary parameters of the inductances and coupling coefficients of the multi-coil transformer can be obtained.

3) Design the geometrical dimensions of the multi-coil transformer layout, and extract the S-parameters by using EM simulation tool.

4) Simulate the S-parameters with the switches to obtain the effective inductance and the tank Q . If necessary, iterations by repeating Items 2-4 above may be carried out to get good agreement with the design targets.

5) Simulate and fit the S-parameters into a wideband lumped circuit model [10], which can be directly used in the Cadence design.

6) Put the circuit model in the designed oscillator and check the performance, including the parasitic extraction of the active devices, switches, and interconnections. Repeat Items 3-6 until the performance is optimized.

To verify the model accuracy of the multi-coil transformer, a testing structure of the layout in Fig. 20 was fabricated and measured. The split transformer can be reconfigured into $N=1$ with the same control signal for D_{0-5} or $N=3$ with $D_0=D_1$, $D_2=D_3$, and $D_4=D_5$ or $N=6$ with different control signals D_{0-5} and $N=6$ with swapping. As shown in Fig. 22, the simulated Q varies from 3.5 to 8.8, while the measured Q varies from 2.6 to 5.3 at 60 GHz. The simulated and measured inductance can be tuned from 22.4-to-31.4 p Ω and 20.4-to-30.5 p Ω , respectively. As summarized in Table II, the measured inductance is slightly shifted down as compared to the

simulated results while the measured Q is smaller compared to the simulated Q due to underestimate of the parasitic loss. Assuming the transformer Q is proportional to its operation frequency, the transformer Q at 95 GHz can be extrapolated to 4.9-to-5.3, which is much smaller than the simulated transformer Q of 7.3-to-9.3, indicating that the parasitic loss is more significant at higher mm-Wave frequencies as expected.

TABLE II. MEASURED TESTING STRUCTURE AT 60 GHz

	Inductance (p Ω)	Q (N=1)	Q (N=3)	Q (N=6)	Q (N=6, swap)
Simulated	22.4~31.4	3.5~8.8	4.2~8.8	4.3~8.8	4.3~8.8
Measured	20.4~30.5	2.6~5.3	3.4~5.3	3.6~5.3	3.8~5.3

VI. CONCLUSIONS

Table III summarizes and compares the performance of the proposed magnetic tuning mm-Wave oscillators with the prior arts. The proposed 70-GHz mm-Wave oscillators demonstrate the widest tuning range and the best FoM_T. Thanks to the proposed split transformer, the W-band DCO achieves the largest tuning range of 27% with the best worst-case FOM_T among all the existing 100-GHz oscillators.

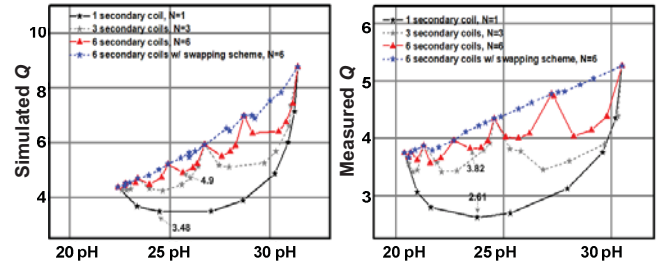


Fig. 22. Simulated and measured Q of the multi-coil transformer at 60 GHz

ACKNOWLEDGMENT

This project is funded by the Hong Kong General Research Fund under the Grant 16208617.

TABLE III. COMPARISON OF MM-WAVE FUNDAMENTAL OSCILLATORS

References	Frequency (GHz)	Tuning Range (GHz)	VDD (V)	Power (mW)	Phase Noise (dBc/Hz)	FoM (dBc/Hz)	FoM _T (dBc/Hz)	Coarse Tuning	Fine Tuning	Process
[17]	61	57-65.5 (14.2%)	1	6	-105.9/ -110.8@10M	-176.2	-179.3	Magnetic	Varactor	65nm CMOS
[24]	56.8	52.2-61.3 (14%)	0.7/1.5	8.7	-94/-118.7@10M	-184.3	-187.4	n.a	Magnetic	90nm CMOS
[16]	62.8	55.1-70.4 (24.6%)	1.2	21.5	-112.2@10M	-174.9	-182.6	Magnetic	Varactor	40nm CMOS
[29]	70.2	62.1-78.3 (22.3%)	1.1	7.7/8.8	-105.8/ -112.0@10M	-180.4	-187.4	Capacitor	Varactor	65nm CMOS
[39]	89.4	87.1-91.7 (5.2%)	1	11	-108.3@10M	-176.9	-171.1	Capacitor	Varactor	65nm CMOS
[22]	101	95.4-106.7 (9.5%)	0.8	11.9	-104.5@10M	-171.1	-176.5	n.a	Magnetic	65nm CMOS
[40]	100.7	98-103.3 (5.2%)	0.8/1.2	12/21	-112.1@10M	-178.6	-172.9	n.a	Active varactor	65nm CMOS
[41]	105	100-110 (9.5%)	1.2	54	-92.8@10M	-175.0	-175.5	n.a	Varactor	65nm CMOS
This Work [18]	73.8	57.5-90.1 (41.1%)	1.2	8.4/10.8	-104.6/ -112.2@10M	-172/ -180	-184.2/ -192.2	Magnetic	Varactor	65nm CMOS
This Work [38]	70	58.8-81.2 (32%)	1	7.2/10	-103.6/ -115.8@10M	-173.5/ -182.3	-183.6/ -192.4	Magnetic	Magnetic	65nm CMOS
This Work [36]	94.8	82-107.6 (27%)	1.2	12	-106/-110@10M	-175.8/ -177.5	-184.4/ -186.1	Magnetic	Magnetic	65nm CMOS
This Work [37]	103.3	95.7-110.5 (14.3%)	1	6.2	-100.6/ -106.9@10M	-172.9/ -178.6	-176/ -181.7	Magnetic	Magnetic	65nm CMOS

REFERENCES

- [1] T. Sowlati et al., "A 60GHz 144-element phased-array transceiver with 51dBm maximum EIRP and $\pm 60^\circ$ beam steering for backhaul application," *IEEE Int. Solid-State Circuits Conf. (ISSCC)*, pp. 66–68, Feb. 2018.
- [2] B. P. Ginsburg et al., "A multimode 76-to-81GHz automotive radar transceiver with autonomous monitoring," *IEEE Int. Solid-State Circuits Conf. (ISSCC)*, pp. 158–160, Feb. 2018.
- [3] P. Peng et al., "A 94 GHz 3D image radar engine with 4TX/4RX beamforming scan technique in 65 nm CMOS technology," *IEEE J. Solid-State Circuits*, vol. 50, no. 3, pp. 656–668, March 2015.
- [4] K. Okada et al., "A 60-GHz 16QAM/8PSK/QPSK/BPSK direct-conversion transceiver for IEEE802.15.3c," *IEEE J. Solid-State Circuits*, vol. 46, no. 12, pp. 2988–3004, Dec. 2011.
- [5] Y. Chao, L. Li and H. C. Luong, "20.3 An 86-to-94.3GHz transmitter with 15.3dBm output power and 9.6% efficiency in 65nm CMOS," *IEEE Int. Solid-State Circuits Conf. (ISSCC)*, pp. 346–347, Feb. 2016.
- [6] X. Yi et al., "A 57.9-to-68.3 GHz 24.6 mW frequency synthesizer with in-phase injection-coupled QVCO in 65 nm CMOS technology," *IEEE J. Solid-State Circuits*, vol. 49, no. 2, pp. 347–359, Feb. 2014.
- [7] S. Kang, J. Chien, and A. M. Niknejad, "A W-band low-noise PLL with a fundamental VCO in SiGe for millimeter-wave applications," *IEEE Trans. Microw. Theory Tech.*, pp. 2390–2404, Oct. 2014.
- [8] S. Rong and H. C. Luong, "Design and analysis of varactor-less interpolative-phase-tuning millimeter-wave LC oscillators with multiphase outputs," *IEEE J. Solid-State Circuits*, vol. 46, no. 8, pp. 1810–1819, Aug. 2011.
- [9] L. Wu and Q. Xue, "E-Band multi-phase LC oscillators with rotated-phase-tuning using implicit phase shifters," *IEEE J. Solid-State Circuits*, vol. 53, no. 9, pp. 2560–2571, Sep. 2018.
- [10] M. Demirkan, S. Bruss and R. Spencer, "Design of wide tuning-range CMOS VCOs using switched coupled-inductors," *IEEE J. Solid-State Circuits*, vol. 43, no. 5, pp. 1156–1163, May 2008.
- [11] M. Vigilante and P. Reynaert, "Analysis and design of an E-Band transformer-coupled low-noise quadrature VCO in 28-nm CMOS," *IEEE Trans. Microw. Theory Tech.*, pp. 1122–1132, April 2016.
- [12] A. I. Hussein, et al., "A 50–66-GHz phase-domain digital frequency synthesizer with low phase noise and low fractional spurs," *IEEE J. Solid-State Circuits*, pp. 3329–3347, Dec. 2017.
- [13] M. Kashani et al., "A wide-tuning-range low-phase-noise mm-Wave CMOS VCO with switchable transformer-based tank," *IEEE Solid-State Circuits Letters*, vol. 1, no. 4, pp. 82–85, April 2018.
- [14] J. Zhang, N. Sharma, and K. K. O, "21.5-to-33.4 GHz voltage-controlled oscillator using NMOS switched inductors in CMOS," *IEEE Microw. Compon. Lett.*, vol. 24, no. 7, pp. 478–480, Jul. 2014.
- [15] P. Agarwal et al., "Switched substrate-shield-based low-loss CMOS inductors for wide tuning range VCOs," *IEEE Trans. Microw. Theory Tech.*, vol. 65, no. 8, pp. 2964–2976, Aug. 2017.
- [16] N. Yanay and E. Socher, "Wide tuning-range mm-Wave voltagecontrolled oscillator employing an artificial magnetic transmission line," *IEEE Trans. Microw. Theory Tech.*, vol. 63, no. 4, pp. 1342–1352, Apr. 2015.
- [17] W. Fei et al., "Design and analysis of wide frequency-tuning-range CMOS 60 GHz VCO by switching inductor loaded transformer," *IEEE Trans. Circuits Syst. I, Reg. Papers*, vol. 61, no. 3, pp. 699–711, Mar. 2014.
- [18] J. Yin and H.C. Luong, "A 57.5–90.1-GHz Magnetically Tuned Multimode CMOS VCO," *IEEE J. Solid-State Circuits*, vol.48, no.8, pp.1851–1861, Aug. 2013.
- [19] K. Kwok, J. R. Long and J. J. Pekarik, "A 23-to-29GHz Differentially Tuned Varactorless VCO in 0.13 μ m CMOS," *IEEE Int. Solid-State Circuits Conf. (ISSCC)*, pp. 194–196, Feb. 2007.
- [20] G. Cusmai et al., "A magnetically tuned quadrature oscillator," *IEEE J. Solid-State Circuits*, vol. 42, pp. 2870–2877, Dec. 2007.
- [21] L. Wu and H. C. Luong, "A 49-to-62 GHz quadrature VCO with bimodal enhanced-magnetic-tuning technique," *IEEE Trans. Circuits Syst. I, Reg. Papers*, vol. 61, pp. 3025–3033, Oct. 2014.
- [22] X. Yi et al., "A 100 GHz transformer-based varactor-less VCO with 11.2% tuning range in 65nm CMOS technology," *IEEE Eur. Solid-State Circuits Conf. (ESSCIRC)*, pp. 293–296, Sep. 2012.
- [23] P. Chiang, O. Momeni and P. Heydari, "A 200-GHz inductively tuned VCO with -7-dBm output power in 130-nm SiGe BiCMOS," *IEEE Trans. Microw. Theory Tech.*, pp. 3666–3673, Oct. 2013.
- [24] T. Lu et al., "Wide tuning range 60 GHz VCO and 40 GHz DCO using single variable inductor," *IEEE Trans. Circuits Syst. I*, vol.60, no.2, pp.257–267, Feb. 2013.
- [25] A. Bevilacqua et al., "Transformer-based dual-mode voltage-controlled oscillators," *IEEE Trans. Circuits Syst. II*, vol. 54, no. 4, pp. 293–297, Apr. 2007.
- [26] S. Rong and H. C. Luong, "Analysis and design of transformer-based dual-band VCO for software-defined radios," *IEEE Trans. Circuits Syst. I*, vol. 59, no. 3, pp. 449–462, Mar. 2012.
- [27] C. H. Hung and R. Gharpurey, "A 57-to-75 GHz dual-mode wide-band reconfigurable oscillator in 65nm CMOS," *IEEE Radio Freq. Integr. Circuits Symp. (RFIC)*, pp. 261–264, June 2014.
- [28] Q. Zou, K. Ma and K. S. Yeo, "A low phase noise and wide tuning range millimeter-wave VCO using switchable coupled VCO-Cores," *IEEE Trans. Circuits Syst. I*, vol. 62, no. 2, pp. 554–563, Feb. 2015.
- [29] Y. Chao and H. C. Luong, "Analysis and design of wide-band millimeter-wave transformer-based VCO and ILFDs," *IEEE Trans. Circuits Syst. I*, vol. 63, no. 9, pp. 1416–1425, Sep. 2016.
- [30] Z. Safarian and H. Hashemi, "Wideband multi-mode CMOS VCO design using coupled inductors," *IEEE Trans. Circuits Syst. I*, vol. 56, no. 8, pp. 1830–1843, Aug. 2009.
- [31] B. Sadhu, M. Ferriss, and A. Valdes-Garcia, "A 52 GHz frequency synthesizer featuring a 2nd harmonic extraction technique that preserves VCO performance," *IEEE J. Solid-State Circuits*, vol. 50, no. 5, pp. 1214–1223, May 2015.
- [32] Z. Zong et al., "A 60 GHz frequency generator based on a 20 GHz oscillator and an implicit multiplier," *IEEE J. Solid-State Circuits*, vol. 51, no. 5, pp. 1261–1273, May 2016.
- [33] A. Shirazi et al., "On the design of mm-Wave self-mixing-VCO architecture for high tuning-range and low phase noise," *IEEE J. Solid-State Circuits*, vol. 51, no. 5, pp. 1210–1222, May 2016.
- [34] J. Yin and H. C. Luong, "A 57.5-to-90.1GHz magnetically-tuned multi-mode CMOS VCO," *IEEE Custom Integrated Circuits Conf. (CICC)*, pp. 1–4, Sep. 2012.
- [35] U. Decanis, et al., "A mm-Wave Quadrature VCO Based on Magnetically Coupled Resonators," *IEEE Int. Solid-State Circuits Conf. (ISSCC)*, pp. 280–281, Feb. 2011.
- [36] Z. Huang and H. C. Luong, "An 82 GHz-to-107.6 GHz Integer-N ADPLL Employing a DCO with Split Transformer and Dual-Path Switched-Capacitor Ladder and a Clock-Skew-Sampling Delta-Sigma TDC," *IEEE J. Solid-State Circuits*, to appear.
- [37] X. Liu et al., "Transformer-based varactor-less 96GHz-110GHz VCO and 89GHz-101GHz QVCO in 65nm CMOS," *IEEE Asian Solid-State Circuits Conf. (ASSCC)*, pp.357–360, Nov. 2016.
- [38] X. Liu, Y. Chao and H. C. Luong, "A 59-to-276 GHz CMOS signal generation for rotational spectroscopy," *IEEE Radio Freq. Integr. Circuits Symp. (RFIC)*, pp. 92–95, June 2017.
- [39] T. Xi et al., "Low-phase-noise 54-GHz transformer-coupled quadrature VCO and 76-/90-GHz VCOs in 65-nm CMOS," *IEEE Trans. Microw. Theory Tech.*, pp. 2091–2103, July 2016.
- [40] S. Kang and A. M. Niknejad, "A 100GHz active-varactor VCO and a bi-directionally injection-locked loop in 65nm CMOS," *IEEE Radio Freq. Integr. Circuits (RFIC)*, pp. 231–234, Jun. 2013.
- [41] M. Adnan and E. Afshari, "A 105GHz VCO with 9.5% tuning range and 2.8mW peak output power using coupled colpitts oscillators in 65nm bulk CMOS," *IEEE Radio Freq. Integr. Circuits (RFIC) Symp.*, pp.239–242, June 2013.